UltraRapid Communication

Proteomic and Metabolomic Analysis of Vascular Smooth Muscle Cells

Role of PKCδ

Manuel Mayr, Richard Siow, Yuen-Li Chung, Ursula Mayr, John R. Griffiths, Qingbo Xu

Abstract—Recent developments of proteomic and metabolomic techniques provide powerful tools for studying molecular mechanisms of cell function. Previously, we demonstrated that neointima formation was markedly increased in vein grafts of PKCδ-deficient mice compared with wild-type controls. To clarify the underlying mechanism, we performed a proteomic and metabolomic analysis of cultured vascular smooth muscle cells (SMCs) derived from PKC$\delta^{+/+}$ and PKC$\delta^{-/-}$ mice. Using 2-dimensional electrophoresis and mass spectrometry, we identified >30 protein species that were altered in PKC$\delta^{-/-}$ SMCs, including enzymes related to glucose and lipid metabolism, glutathione recycling, chaperones, and cytoskeletal proteins. Interestingly, nuclear magnetic resonance spectroscopy confirmed marked changes in glucose metabolism in PKC$\delta^{-/-}$ SMCs, which were associated with a significant increase in cellular glutathione levels resulting in resistance to cell death induced by oxidative stress. Furthermore, PKC$\delta^{-/-}$ SMCs overexpressed RhoGDIα, an endogenous inhibitor of Rho signaling pathways. Inhibition of Rho signaling was associated with a loss of stress fiber formation and decreased expression of SMC differentiation markers. Thus, we performed the first combined proteomic and metabolomic study in vascular SMCs and demonstrate that PKCδ is crucial in regulating glucose and lipid metabolism, controlling the cellular redox state, and maintaining SMC differentiation. **(*Circ Res*. 2004;94:e87-e96.)**

Key Words: proteomics ■ metabolomics ■ smooth muscle cells ■ PKC ■ signal transduction

Proteomic and metabolomic techniques are ideal for clarifying quantitative protein and metabolite changes in physiological and diseased conditions, respectively.[1–5] In vascular research, however, proteomics and metabolomics are still in their infancies[6–8] and no studies have been performed so far comparing proteomic and metabolomic profiles in vascular smooth muscle cells (SMCs).

PKCδ represents a novel PKC isoform as characterized on the basis of its structure and maximal activation by diacylglycerol in the absence of calcium.[9,10] We recently developed knockout mice lacking PKCδ and studied its effect on neointima formation in vein grafts.[11] We demonstrated that loss of PKCδ markedly accelerated neointima formation, resulting in complete occlusion of the vessel lumen in one-third of the vein grafts. As with p53-deficient mice,[12] neointimal lesions in PKC$\delta^{-/-}$ vein grafts contained twice as many SMCs as wild-type controls and showed significantly lower numbers of apoptotic SMCs.[11] In vitro experiments revealed that SMCs derived from PKC$\delta^{-/-}$ mice were less sensitive to various apoptotic stimuli, including cytokine treatment. Their apoptotic resistance appeared to involve a loss of free radical generation as evidenced by redox-sensitive fluorescent dyes.[11] Besides modulating apoptosis, PKCδ was found to be important for cytoskeleton rearrangement and cell migration.[13] However, the molecular mechanisms of resistance to apoptosis and cytoskeletal abnormalities in PKC$\delta^{-/-}$ SMCs are unknown. In the present study, we performed a thorough analysis of the proteome and metabolome of vascular SMCs derived from PKC$\delta^{+/+}$ and PKC$\delta^{-/-}$ mice. We demonstrate that PKCδ is crucial for SMC homeostasis by regulating the balance between glucose and lipid metabolism and maintaining SMC differentiation.

Materials and Methods

All procedures were performed according to protocols approved by the Institutional Committee for Use and Care of Laboratory Animals. PKCδ-deficient mice were generated by targeted disruption of an endogenous PKCδ gene.[11] Vascular SMCs from PKC$\delta^{-/-}$ and PKC$\delta^{+/+}$ mice were cultivated from aortas of 5 different animals, SMCs from PKC$\delta^{+/-}$ mice were cultivated from aortas of 3 different animals, as described elsewhere.[14]

Proteomic Analysis

Protein extracts of PKC$\delta^{-/-}$ and PKC$\delta^{+/+}$ SMCs were separated by 2-dimensional gel electrophoresis (2-DE) as described by McGregor et al.[15] Spot patterns were analyzed using Proteomweaver 2.0

Received December 22, 2003; revision received April 23, 2004; accepted April 27, 2004.

From the Department of Cardiac and Vascular Sciences (M.M., U.M., Q.X.) and Department of Basic Medical Sciences (Y.-L.C., J.R.G.), St George's Hospital Medical School, London, UK; and Centre for Cardiovascular Biology and Medicine (R.S.), King's College, London, UK.

Correspondence to Prof Qingbo Xu, Department of Cardiac and Vascular Sciences, St George's Hospital Medical School, Cranmer Terrace, London SW17 0RE, UK. E-mail q.xu@sghms.ac.uk

Circulation Research **is available at http://www.circresaha.org** **DOI: 10.1161/01.RES.0000131496.49135.1d**

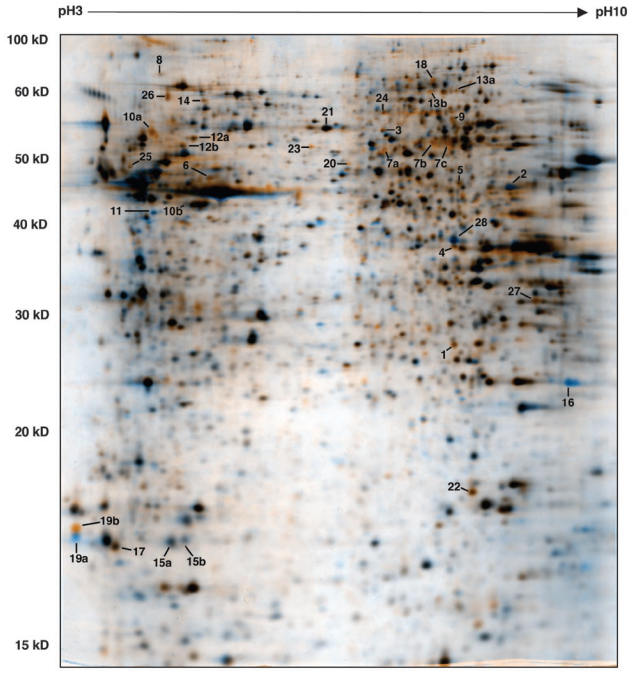

Figure 1. 2-DE map of SMC proteins. Protein extracts were separated on a pH 3 to 10 NL IPG strip, followed by a 12% SDS polyacrylamide gel. Spots were detected by silver staining. Figures represent a direct overlay of average gels from PKC$\delta^{+/+}$ and PKC$\delta^{-/-}$ SMCs. Each average gel was created from 4 single gels (total n=8). Differentially expressed spots are highlighted in color (blue and orange for PKC$\delta^{+/+}$ and PKC$\delta^{-/-}$ SMCs, respectively). Proteins identified by MALDI-MS are marked with numbers and listed in Table 1.

(Definiens) and PDQuest Software 7.1 (Biorad). Spots showing a statistically significant difference in intensity were excised for identification by matrix-assisted laser desorption ionization mass spectrometry (MALDI-MS) or tandem mass spectrometry (MS/MS). A detailed methodology is provided in the online data supplement available at http://circres.ahajournals.org.

Proton Magnetic Resonance Spectroscopy

SMC monolayers were washed twice with chilled saline and SMC metabolites were extracted in 6% perchloric acid.[16] Neutralized extracts were freeze-dried and reconstituted in D_2O; 0.5 mL of the extracts were placed in 5 mm proton nuclear magnetic resonance (NMR) tubes. ^{1}H NMR spectra were obtained using a Bruker 500 MHz spectrometer. The water resonance was suppressed by using gated irradiation centered on the water frequency. Sodium 3-trimethylsilyl-2,2,3,3-tetradeuteropropionate (TSP) was added to the samples for chemical shift calibration and quantification. Immediately before the NMR analysis, the pH was readjusted to 7 with perchloric acid or KOH.

Standard Biochemical Methods

The methodology for reverse-transcriptase polymerase chain reaction (RT-PCR), Western blotting, Rho-activation assays, cell viability, and spreading assays is provided in the online data supplement (http://www.circresaha.org).

Statistical Analysis

Statistical analysis was performed using the analysis of variance and Student *t* test, respectively. The association of SMC metabolites with PKCδ genotypes was assessed using generalized linear models. Results were given as means±SE. A $P<0.05$ was considered significant.

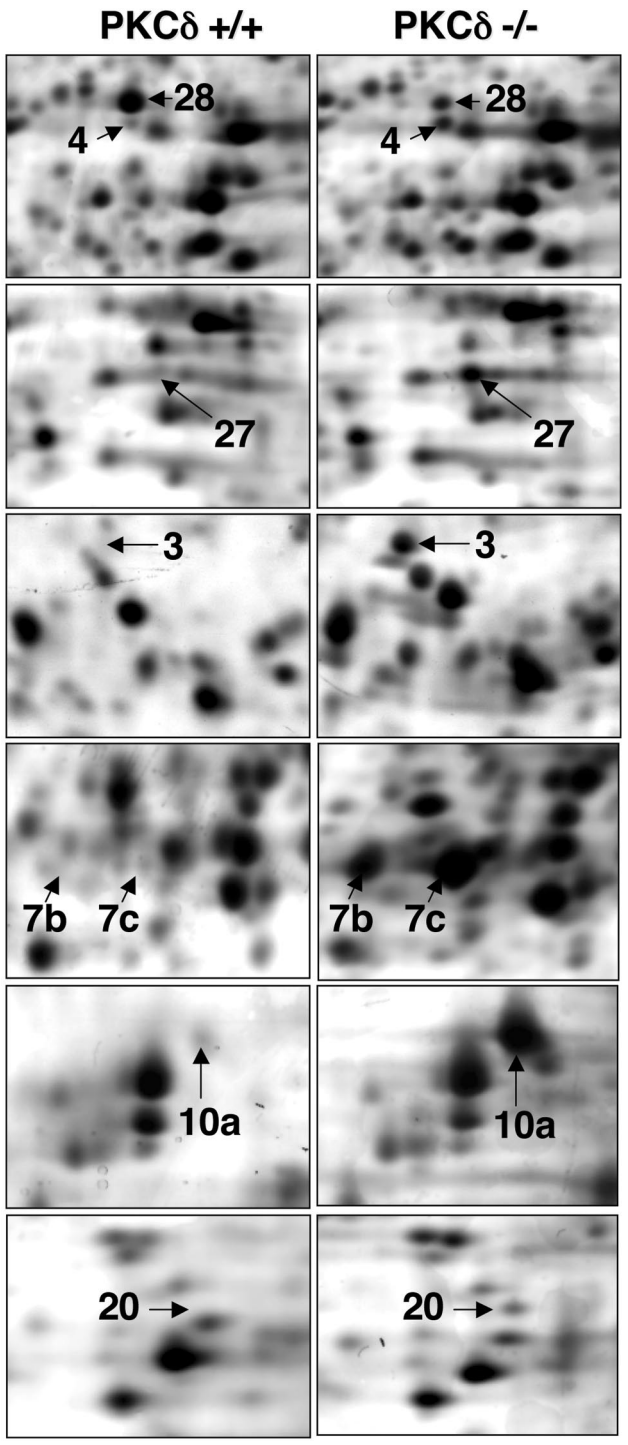

Figure 2. Enlargements of silver stained gels. Representative areas of 2-dimensional gels from wild-type and PKC$^{-/-}$ SMCs highlight quantitative differences in images. Numbers correspond to proteins listed in Table 1.

Results

Proteomic Analysis

To analyze changes in the proteome, we created a protein profile of SMCs by 2-DE. Average gels for PKC$\delta^{+/+}$ and PKC$\delta^{-/-}$ SMCs were obtained from cultures obtained from 4 different animals per group (mean passage 25±3 and 26±4 for PKC$\delta^{+/+}$ and PKC$\delta^{-/-}$ SMCs, respectively). A direct

TABLE 1. Differences in Protein Profiles Between Vascular SMCs of PKC$\delta^{+/+}$ and PKC$\delta^{-/-}$ Mice

N	Protein Identity	Δ	*P*	NCBI Entry Number	Function	Calculated pI/MM* (*Da*×10^3)	Observed pI/MM (*Da*×10^3)	Sequence Coverage/ Mascot Score
	Energy Metabolism							
1	Triose phosphate isomerase	+2.2	0.040	12846508	Glycolysis	6.9/26.7	6.9/26.8	24/62†
2	Phosphoglycerate kinase 1	+1.5	0.005	20844750	Glycolysis	8.0/44.5	7.8/47.1	30/101†
3	Glucose 6-phosphate dehydrogenase	+4.0	0.012	6996917	Pentose phosphate pathway	6.1/59.2	6.4/56.5	38/229
4	Aldose reductase	+7.7	0.001	3046247	Sorbitol pathway	6.7/35.7	6.9/37.6	31/105
5	Isocitrate dehydrogenase, soluble	+3.2	0.048	6754278	NADPH generation	6.5/46.6	6.9/47.1	19/76
6	Acyl-CoA dehydrogenase, short/branched chain	+3.0	0.007	17647119	Fatty acid oxidation	8.0/47.8	5.1/47.7	16/84
7a	Alcohol dehydrogenase 3, A1	>+10	0.000	6680676	Aldehyde dehydrogenase	6.5/50.4	6.4/52.7	8/68
7b	Alcohol dehydrogenase 3, A1	+5.7	0.001	6680676	Aldehyde dehydrogenase	6.5/50.4	6.8/54.1	22/113
7c	Alcohol dehydrogenase 3, A1	+4.0	0.030	6680676	Aldehyde dehydrogenase	6.5/50.4	6.9/54.7	30/224
	Chaperones							
8	Heat shock protein 4	+2.1	0.037	13277753	Heat shock protein 70 kDa	5.1/94.0	4.7/78.8	12/85
9	CCT-1 subunit zeta, 6a	+4.4	0.009	6753324	T-complex polypeptide 1	6.6/58.0	6.9/58.4	12/64
10a	Protein disulfide isomerase precursor	+4.5	0.045	129729	Prolyl 4-hydroxylase beta	4.8/57.1	4.7/56.2	26/124
10b	Protein disulfide isomerase precursor	+3.6	0.028	129729	Prolyl 4-hydroxylase beta	4.8/57.1	5.0/43.1	17/88
	Cytoskeleton							
11	Vimentin	−3.3	0.000	2078001	Intermediate filament	5.0/51.5	4.7/42.1	20/90
12a	Vimentin	+6.5	0.043	2078001	Intermediate filament	5.0/51.5	4.9/53.5	47/187†
12b	Vimentin	+8.7	0.048	2078001	Intermediate filament	5.0/51.5	5.0/55.0	33/156†
13a	Lamin A	+3.2	0.001	1346412	Intermediate filament	6.5/74.2	6.9/65.5	12/84
13b	Lamin A	>+10	0.000	1346412	Intermediate filament	6.5/74.2	6.7/64.9	33/242
14	Lamin B	+2.3	0.019	110630	Intermediate filament	5.1/66.2	5.1/62.8	16/81
15a	Actin	−2.8	0.008	553859	Myofilaments	5.3/16.8	4.8/16.7	39/79
15b	Actin	−2.3	0.028	553859	Myofilaments	5.3/16.8	4.9/16.7	31/70
16	SM22 alpha	<−10	0.000	6755714	Transgelin	8.9/22.6	8.9/22.6	64/210†
17	Myosin alkali light chain, Smooth-muscle isoform	+2.5	0.012	127148	Myofilaments	4.5/17.0	4.4/16.6	39/114
18	Caldesmon 1	+3.7	0.015	21704156	Myofilaments	7.0/60.4	6.8/67.9	19/78†
19a	Calmodulin	<−10	0.048	4502549	Phosphorylase kinase delta	4.1/16.8	4.1/16.9	33/62
19b	Calmodulin	>+10	0.030	4502549	Phosphorylase kinase delta	4.1/16.8	4.1/16.8	36/63
20	Tubulin alpha	>+10	0.000	6678469	Microtubules	4.9/49.8	6.1/49.6	23/78
	Others							
21	Glucose-regulated protein	+1.5	0.049	26353794	Phospholipase C alpha, contains thioredoxin	6.0/56.6	6.0/56.5	27/112
22	Mixture: components	+2.1	0.038					mixture: 156
	1) Glutathione S-transferase			6754086	1) Conjugation of GSH	6.8/26.6		41/70
	2) Expressed in nonmetastatic cells			6679078	2) Nucleoside diphosphate kinase B	7.0/17.4	7.0/17.6	61/88†
23	Septin 8	+4.7	0.001	23621405	Cell division	5.7/49.8	5.9/52.8	18/97
24	Collapsin response mediator protein 2	+3.5	0.000	6753676	Dihydropyrimidine-like 2 protein	6.0/62.1	6.5/60.5	15/82
25	Angiogenin inhibitor 1	+2.8	0.008	16307569	Ribonuclease	4.7/49.8	4.5/49.6	15/62
26	Fkbp9 protein	+2.6	0.027	20072768	Peptidyl-prolyl cis-trans isomerase	5.0/63.4	4.8/63.3	11/121
27	Carbohydrate binding protein 35	+4.8	0.000	387111	Lectin	9.0/27.6	8.3/31.3	29/84
28	Annexin 1	−4.2	0.007	113945	Lipocortin 1, calpactin II	7.0/38.7	6.9/38.5	46/188†

Δ indicates fold increased/decreased expression in PKC$\delta^{-/-}$ SMCs compared to PKC$\delta^{+/+}$ SMCs.

*pI/MM, isoelectric point/molecular mass.

†Additional verification by MS/MS.

TABLE 2. Protein Identification by Tandem MS

N	Protein Identity	SWISS-PROT Entry Name	SWISS-PROT Primary Accession Number	Peptide Matches	Sequence	Sequence Coverage (%)
1	Triose phosphate isomerase	TPIS_MOUSE	P17751	9	(K)FFVGG NWK(M)	55.65
					(K)VIADN VKDWS K(V)	
					(R)IIYGG SVTGA TCK(E)	
					(K)TATPQ QAQEV HEK(L)	
					(K)DLGAT WVVLG HSER(R)	
					(K)VVLAY EPVWA IGTGK(T)	
					(K)VTNGA FTGEI SPGMI K(D)	
					(K)VSHAL AEGLG VIACI GEK(L)	
					(K)ELASQ PDVDG FLVGG ASLKP EFVDI INAK(Q)	
2	Phosphoglycerate kinase 1	PGK1_MOUSE	P09411	3	(R)GCITI IGGGD TATCC AK(W)	12.74
					(K)ITLPV DFVTA DKFDE NAK(T)	
					(K)QIVWN GPVGV FEWEA FAR(G)	
12a	Vimentin	VIME_MOUSE	P20152	4	(R)SYVTT STR(T)	13.98
					(R)ISLPL PTFSS LNLR(E)	
					(R)QVQSL TCEVD ALKGT NESLE R(Q)	
					(R)LLQDS VDFSL ADAIN TEFKN TR(T)	
12b	Vimentin	VIME_MOUSE	P20152	9	(R)FLEQQ NK(I)	27.53
					(R)SLYSS SPGGA YVTR(S)	
					(R)KVESL QEEIA FLK(K)	
					(R)ISLPL PTFSS LNLR(E)	
					(K)FADLS EAANR NNDAL R(Q)	
					(R)LLQDS VDFSL ADAIN TEFK(N)	
					(R)EEAES TLQSF RQDVD NASLA R(L)	
					(R)QVQSL TCEVD ALKGT NESLE R(Q)	
					(R)LLQDS VDFSL ADAIN TEFKN TR(T)	
16	SM22 alpha, transgelin	TAGL_MOUSE	P37804	2	(R)DFTDS QLQEG K (H)	14.50
					(R)LVEWI VVQCG PDVGR PDR(G)	
18	Similar to caldesmon 1	Q8VCQ8	Q8VCQ8	1	(K)IDSRL EQYTN AIEGT K(A)	3.02
22	Nucleoside diphosphate kinase B	NDKB_MOUSE	Q01768	2	(K)DRPFF PGLVK(Y)	16.45
					(K)EIHLW FKPEE LIDYK(S)	
28	Annexin 1	ANX1_MOUSE	P10107	9	(R)SNEQI REINR(V)	35.65
					(K)CATST PAFFA EK(L)	
					(K)ALDLE LKGDI EK(C)	
					(K)YGISL CQAIL DETK(G)	
					(R)FLENQ EQEYV QAVK(S)	
					(K)GLGTD EDTLI EILTT R(S)	
					(R)KALTG HLEEV VLAML K(T)	
					(K)YGISL CQAIL DETKG DYEK(I)	
					(K)GGPGS AVSPY PSFNV SSDVA ALHK(A)	

overlay is presented in Figure 1. Using a broad range pH gradient (pH 3 to 10 NL), 2-DE gels compromised ≈1200 protein features. Differentially expressed spots are highlighted in color (blue and orange indicate an increase in PKC$\delta^{+/+}$ and PKC$\delta^{-/-}$ SMCs, respectively). Enlarged silver-stained gels highlight quantitative differences in images (Figure 2). Numbered spots were excised and subject to in-gel tryptic digestion. Protein identifications as obtained by MALDI-MS are listed in Table 1. For proteins marked with a dagger in Table 1, further proof of identification was obtained by tandem mass spectrometry (Table 2). A representative MALDI-MS spectrum is shown in Figure 3.

Strikingly, many changes observed in PKC$\delta^{-/-}$ SMCs were related to energy metabolism, including enzymes involved in glucose and lipid metabolism: triose phosphate isomerase and phosphoglycerate kinase represent glycolytic enzymes, whereas glucose 6-phosphate dehydrogenase and aldose reductase are the rate-limiting enzymes in the pentose phosphate and sorbitol path-

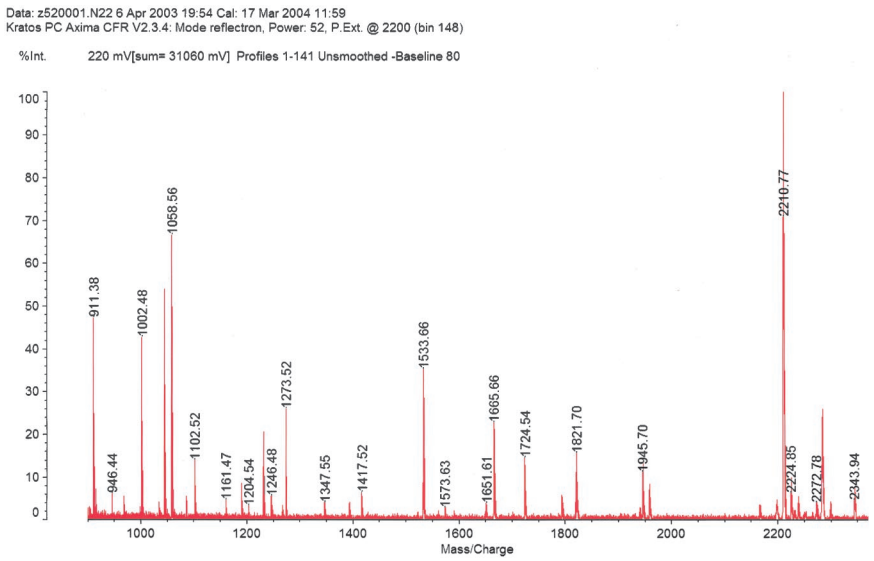

Figure 3. Mass spectrometry spectrum. Peptide mass profiling of a silver-stained spot from a 2-DE separation of murine SMC proteins. The protein of spot 3 (Figure 1) was digested in situ within the gel with trypsin. The resulting tryptic peptides were analyzed using MALDI-MS in reflectron mode. The protein was identified as glucose 6-phosphate dehydrogenase (Table 1).

ways, respectively. Concomitantly, 3 isoforms of aldehyde dehydrogenase 3A1 and a highly acidic isoform of acyl-CoA dehydrogenases were found only in PKCδ$^{-/-}$, but not in PKCδ$^{+/+}$ SMCs (Table 1). Additionally, the soluble form of the isocitrate dehydrogenase, which has recently been implicated in glutathione (GSH) recycling,[17] appeared to be upregulated in PKCδ$^{-/-}$ SMCs.

Besides enzymatic alterations, we observed profound changes in cytoskeletal proteins in PKCδ$^{-/-}$ SMCs, including actin and myosin light chain, which were associated with a compensatory increase in intermediate filaments, eg, vimentin and lamin, and alterations in calcium binding proteins, eg, calmodulin and caldesmon 1 (Table 1). Moreover, PKCδ deficiency resulted in marked changes of cellular chaperones, including heat shock protein 4 (Hsp4), the tubulin binding-subunit of the T-complex polypeptide 1 (CCT-1ζ),[18] and the redox sensitive chaperone protein disulfide isomerase.[19,20] Further alterations were observed for proteins involved in cell division, eg, septin and immunoregulation, eg, Fkbp9 and annexin 1. Taken together, our proteomic data suggest that PKCδ deficiency is associated with altered energy generation and cytoskeletal dysregulation in vascular SMCs.

Metabolomic Analysis

To prove the functional relevance of the described enzymatic changes, we applied high-resolution NMR spectroscopy to analyze cellular metabolites (Figure 4). In PKCδ$^{+/-}$ and PKCδ$^{-/-}$ SMCs levels of alanine, a surrogate marker for the activity of the glycolytic pathway in metabolomic analysis were significantly decreased (Table 3, Figure 5A), whereas lactate tended to accumulate, indicating impaired glucose metabolism. Notably, carnitine, required for the mitochondrial import of long chain fatty acids, was markedly elevated in PKCδ$^{-/-}$ SMCs and associated with higher levels of phosphocholine, an essential phospholipid for the synthesis of cell membranes. The metabolic changes in PKCδ$^{-/-}$ SMCs resulted in an accumulation of amino acids, such as glutamate, valine, isoleucine, and a diminished creatine pool, a major energy reserve in muscle tissue. ATP levels were similar to PKCδ$^{+/+}$ SMCs when cells were grown in high glucose medium (25 mmol/L) but significantly decreased under normal glucose concentrations (5 mmol/L) (Figure 5B; 90 versus 65 μmol ATP/g protein, $P<0.05$). Thus, higher levels of glucose are required to maintain cellular energy production in the absence of PKCδ.

Elevated Glutathione Levels Protect PKCδ$^{-/-}$ SMCs

One of the most prominent enzymatic changes in PKCδ$^{-/-}$ SMCs were observed for the soluble form of isocitrate dehydrogenase and glucose 6-phosphate dehydrogenase, 2 enzymes related to GSH metabolism. This prompted us to measure GSH concentrations (Figure 5C): PKCδ deficiency was associated with a significant increase in GSH levels (25 versus 70 μmol/g protein, $P<0.001$). The difference to PKCδ$^{+/+}$ SMCs was less pronounced under high glucose conditions (15 versus 22 μmol/g protein, $P<0.01$), which represents a considerable oxidative stress leading to GSH consumption.[21,22]

GSH is a tripeptide with a free sulfhydryl group and is of paramount importance in maintaining the reducing intracellular environment.[21,23] Consequently, increased GSH protected PKCδ$^{-/-}$ SMCs against oxidative stress-induced cell death: treatment with 100 μmol/L diethylmaleate (DEM), a sulfhydryl-reactive agent, resulted in rapid depletion of GSH (Figure 6A), followed by a drop in ATP levels (Figure 6B) and cell death in PKCδ$^{+/+}$ SMCs (Figure 6C). In contrast, PKCδ$^{-/-}$ SMCs were less sensitive to DEM-induced cell death (Figure 6A to C), tolerating up to 20-times higher concentrations of DEM than PKCδ$^{+/+}$ SMCs (data not shown). Corresponding to GSH depletion, the antioxidant protein heme oxygenase 1 (HO-1) was rapidly induced in PKCδ$^{+/+}$, but not in PKCδ$^{-/-}$ SMCs (Figure 6D). Differences in HO-1 expression were restricted to oxidative stress, because HO-1 expression after exposure to heavy metals, eg, cadmium chloride ($CdCl_2$), was similar in PKCδ$^{+/+}$ and PKCδ$^{-/-}$ SMCs (Figure 6E). Taken together, our data clearly demonstrate that loss of PKCδ alters the cellular redox state by elevating GSH levels, providing protection against oxidative stress-induced cell death.

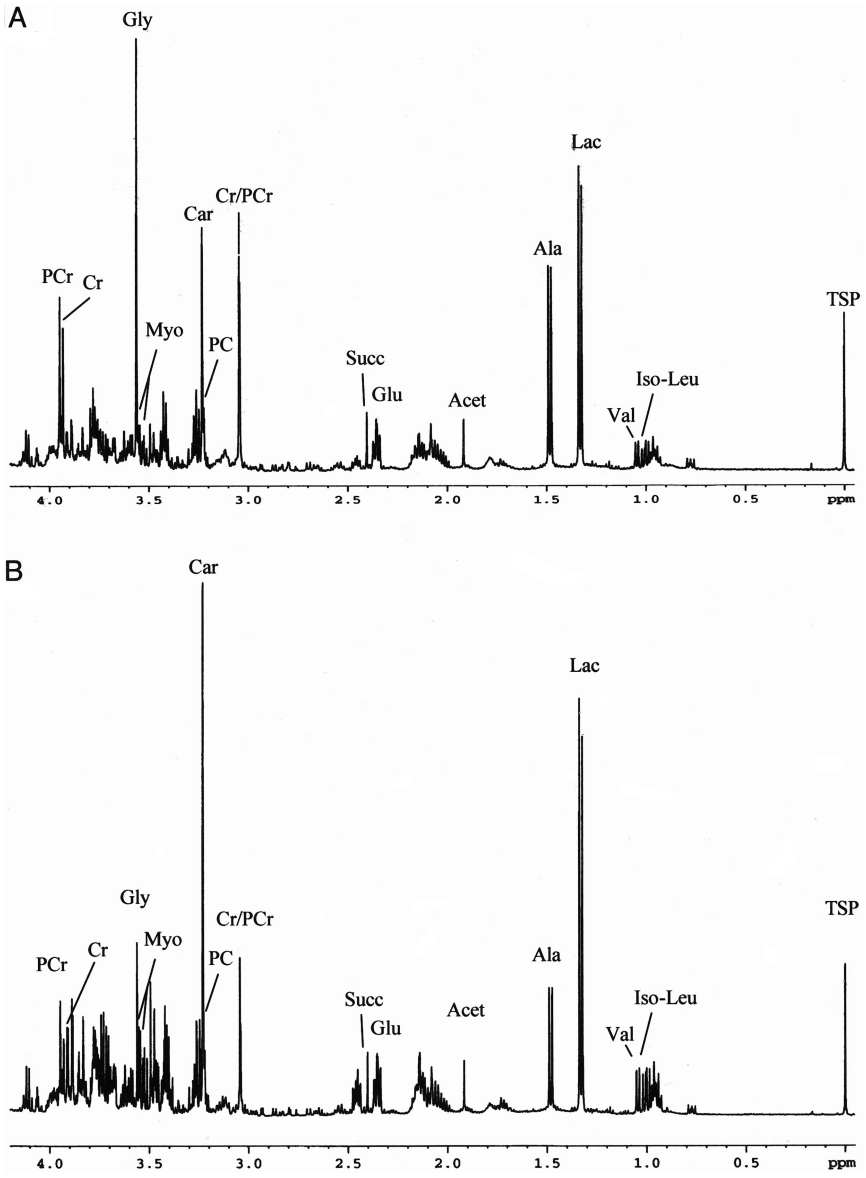

Figure 4. NMR spectra of PKC$\delta^{+/+}$ (A) and PKC$\delta^{-/-}$ SMCs (B). Resonances have been assigned to alanine (Ala), creatine 2 (Cr), phosphocreatine (PCr), carnitine (Car), phosphocholine (PC), glutamate (Glu), lactate (Lac), acetate (Acet), succinate (Suc), glycine (Gly), myoinositol (Myo), valine (Val), and isoleucine (Iso-Leu). Sodium 3-trimethylsilyl-2,2,3,3-tetradeuteropropionate (TSP) was added to the samples for calibration.

Impaired Rho Signaling in PKC$\delta^{-/-}$ SMCs

In addition to using a wide-range pH gradient (pH 3 to 10 NL), we separated proteins on a pH 4 to 7 gradient (data not shown). Because the same amount of protein was used for all analytical gels, only the spatial resolution was superior compared with the pH3–10 NL gradient. Using this gradient, we observed differential expression for Rho guanine dissociation inhibitor alpha (RhoGDIα) (Figure 7A), an endogenous inhibitor of RhoGTPases including Rho, Rac, and Cdc42,[24] which orchestrate the regulation of actin polymerization.[25] We explored its functional relevance by Western blotting and immunoprecipitation of activated Rho (RhoGTP): increased expression of RhoGDIα in PKC$\delta^{-/-}$ SMCs (Figure 7B) attenuated Rho activation in response to mechanical stress (Figure 7C, D).

Loss of PKCδ Causes SMC Dedifferentiation

The small GTPases of the Rho/Rac family orchestrate the regulation of p38MAPK pathways and actin polymerization.[25–28] Cytoskeletal dynamics[29] and organization play a crucial role in maintaining SMC differentiation.[30,31] Impaired Rho signaling in PKCδ deficient SMCs was associated with a disassembly of stress fibers (Figure 8A). Additionally, decreased abundance of the differentiation marker SM22α in the proteomic profile suggested a phenotypic modulation (spot 16, Table 1). This was further investigated by use of RT-PCR analysis: loss of PKCδ was associated with transcriptional downregulation of SM22α (Figure 8B). Similarly, lower expression levels were observed for SM myosin heavy chain (SMMHC) and calponin (Figure 8C), but not α-SM actin (Figure 8B). Thus, inhibition of Rho signaling in PKC$\delta^{-/-}$ SMCs is associated with a loss of cytoskeletal organization resulting in SMC dedifferentiation.

Discussion

The present study provides the first proteomic profile of murine vascular SMCs that was markedly influenced by mutational ablation of the PKCδ gene. Importantly, pro-

TABLE 3. Metabolic Effects of PKCδ Deficiency in Vascular SMCs

	PKCδ$^{+/+}$	PKCδ$^{+/-}$	PKCδ$^{-/-}$	*P* (ANOVA)	*P* (Linear Trend)
Alanine	149.47 (±9.75)	**108.70 (±5.60)**	**91.75 (±10.52)**	**0.001**	**0.000**
Lactate	351.35 (±61.35)	414.14 (±94.93)	508.75 (±114.91)	0.466	0.213
Glutamate	60.10 (±4.86)	60.48 (±4.12)	**80.91 (±7.11)**	**0.031**	**0.018**
Valine	28.34 (±3.71)	31.33 (±4.61)	**53.22 (±12.16)**	**0.096**	**0.041**
Isoleucine	21.52 (±3.13)	27.34 (±3.65)	**46.60 (±10.79)**	**0.060**	**0.021**
Carnitine	22.82 (±4.67)	23.45 (±4.11)	**43.53 (±3.95)**	**0.004**	**0.003**
Acetate	23.17 (±4.63)	26.34 (±8.05)	31.47 (±7.43)	0.645	0.345
Succinate	11.99 (±2.22)	8.95 (±0.96)	13.86 (±1.63)	0.249	0.478
Myoinositol	82.75 (±11.14)	119.56 (±10.44)	155.62 (±49.66)	0.297	0.114
Choline	1.50 (±0.18)	2.39 (±0.97)	2.47 (±1.31)	0.321	0.159
Phosphocholine	5.92 (±0.52)	6.76 (±1.38)	**10.81 (±1.79)**	**0.035**	**0.013**
Total Creatine	74.95 (±7.27)	**45.64 (±3.12)**	**53.70 (±3.28)**	**0.004**	**0.017**
Glycine	110.80 (±2.56)	114.44 (±10.09)	85.23 (±13.77)	0.109	**0.076**

Data presented are given in μmol/g protein (mean±SE, n=4 biological replicates in each group, except for PKCδ$^{+/-}$ SMCs n=3, measurements were performed in duplicates, total n=22).

P values for differences between the 3 groups were derived from ANOVA tables (bold numbers highlight significant differences from wild-type controls in the Fisher PLSD test), *P* values for the linear trend are listed in the far right column.

teomic findings were translated into a functional context by combining proteomic techniques with NMR spectroscopy. This new research strategy allows us to decipher the effects of specific genes, drugs, or other treatments on global alterations of cellular proteins, metabolism and function.

Most of our knowledge about the role of PKCδ is derived from studies using rottlerin, a putative PKCδ inhibitor.[13,32,33]

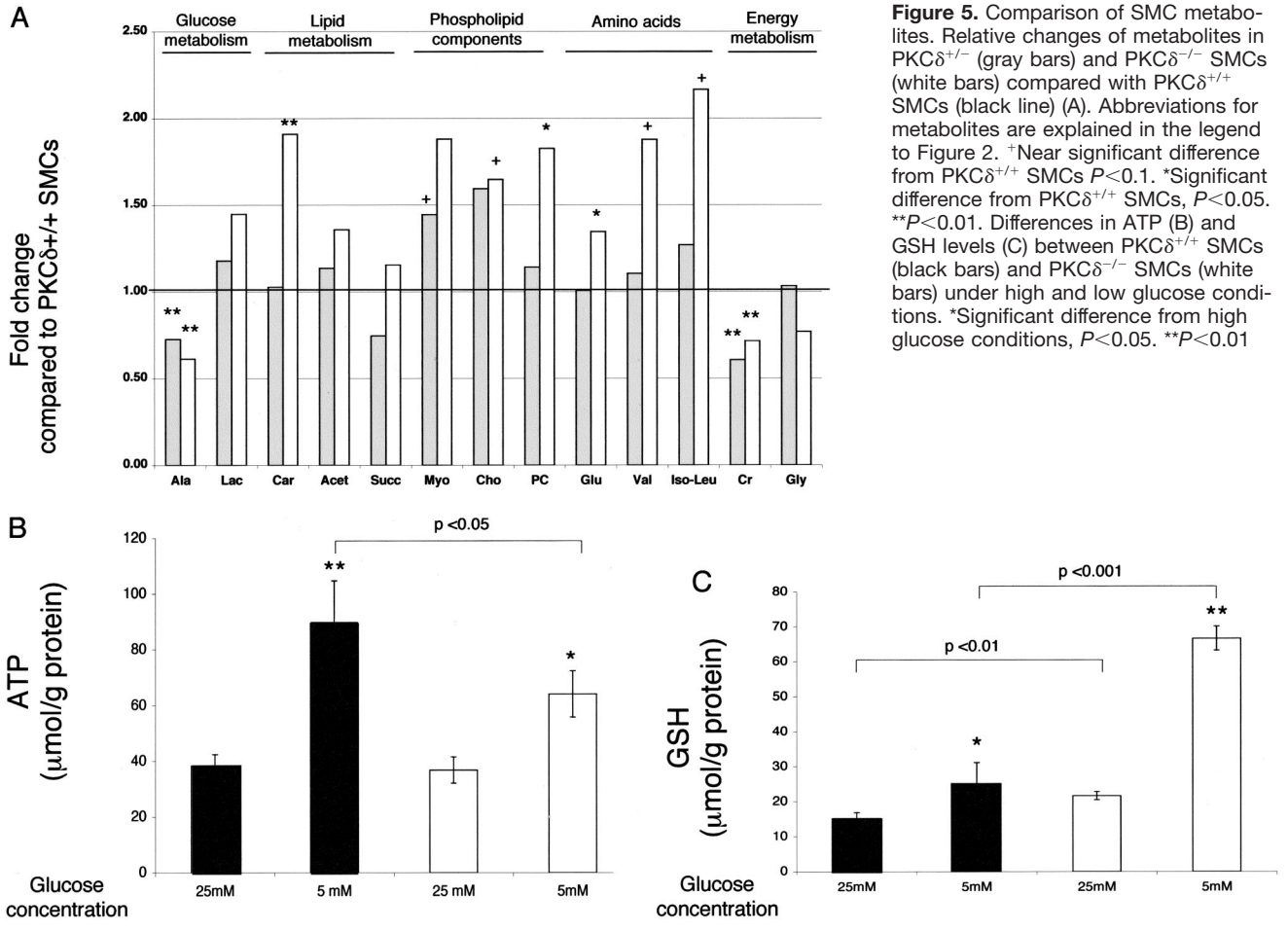

Figure 5. Comparison of SMC metabolites. Relative changes of metabolites in PKCδ$^{+/-}$ (gray bars) and PKCδ$^{-/-}$ SMCs (white bars) compared with PKCδ$^{+/+}$ SMCs (black line) (A). Abbreviations for metabolites are explained in the legend to Figure 2. $^{+}$Near significant difference from PKCδ$^{+/+}$ SMCs $P<0.1$. *Significant difference from PKCδ$^{+/+}$ SMCs, $P<0.05$. **$P<0.01$. Differences in ATP (B) and GSH levels (C) between PKCδ$^{+/+}$ SMCs (black bars) and PKCδ$^{-/-}$ SMCs (white bars) under high and low glucose conditions. *Significant difference from high glucose conditions, $P<0.05$. **$P<0.01$

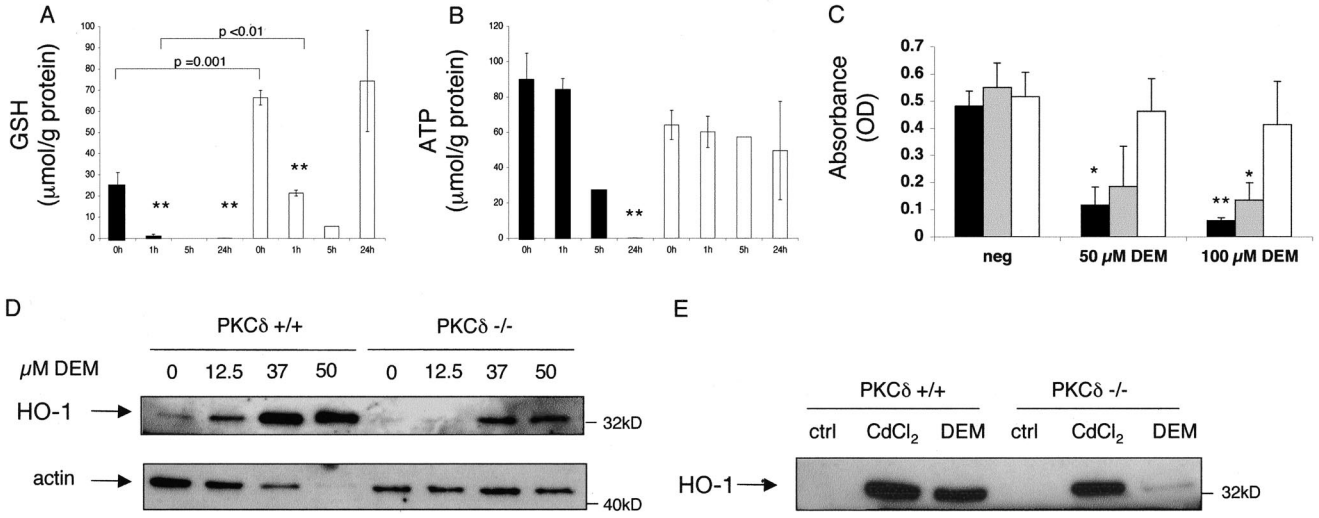

Figure 6. Increased resistance to oxidative stress-induced cell death in PKC$\delta^{-/-}$ SMCs. PKC$\delta^{+/+}$ SMCs (black bars) and PKC$\delta^{-/-}$ SMCs (white bars) were treated with 100 μmol/L diethylmaleate (DEM). GSH (A) and ATP (B) concentrations were measured at the indicated time-points and SMC survival was quantified after 24 hours using a proliferation/cell death kit (Promega). Black, gray, and white bars represent absorbance values for PKC$\delta^{+/+}$ SMCs, PKC$\delta^{+/-}$, and PKC$\delta^{-/-}$ SMCs, respectively (C). *Significant difference from controls $P<0.05$, **$P<0.01$. DEM-induced expression of heme oxygenase-1 (HO-1) in PKC$\delta^{+/+}$ and PKC$\delta^{-/-}$ SMCs (n=5) (D). Note that the decrease in actin in PKC$\delta^{+/+}$ SMCs is a consequence of increased cell death. Comparison of HO-1 induction in PKC$\delta^{+/+}$ and PKC$\delta^{-/-}$ SMCs after treatment with DEM (50 μmol/L) and cadmium chloride ($CdCl_2$, 10 μmol/L) (n=3) (E).

However, its specificity has recently been questioned as it appears to block PKCδ activity indirectly in vivo by uncoupling mitochondria.[34] In the present study, we delineate the effects of PKCδ on vascular SMCs by using PKC$\delta^{-/-}$ mice. Our proteomic and metabolomic data suggest that loss of PKCδ interferes with glucose metabolism, affecting energy reserves and promoting an antioxidant state of cells reflected by decreased levels of intracellular reactive oxygen species[11] and increased GSH concentrations. GSH turnover was more efficient in PKC$\delta^{-/-}$ SMCs after DEM treatment and provided protection against oxidative stress-induced cell death.

Our metabolomic findings are in line with a recent study by Caruso et al[33] demonstrating that PKCδ is required for stimulation of the pyruvate dehydrogenase complex. Pyruvate dehydrogenase catalyzes the oxidation of pyruvate to acetyl-CoA, which represents the irreversible step from glycolysis to the citric acid cycle. SMC metabolism, when viewed in terms of ATP synthesis, is primarily oxidative, with glucose being the main source of energy for contractile energy requirements, whereas aerobic lactate production appears to be specifically coupled to sodium and potassium transport processes.[35,36] Hence, decreased activity of the pyruvate dehydrogenase complex in the absence of PKCδ provides a likely explanation for the diminished creatine pool and reduced ATP levels at 5 mmol/L glucose. Impaired glucose metabolism in PKC$\delta^{-/-}$ SMCs was reflected as a decrease in alanine, accumulation of lactate, decreased oxidation of certain amino acids, and compensatory upregulation of alternative metabolic pathways. First, lipid metabolism was increased as evidenced by proteomic changes in acyl-CoA dehydrogenase and aldehyde dehydrogenase 3A1 and a corresponding elevation of carnitine and phosphocholine, the precursor for phosphatidylcholine. The biosynthesis of phosphatidylcholine is driven by the availability of free fatty acids, which are

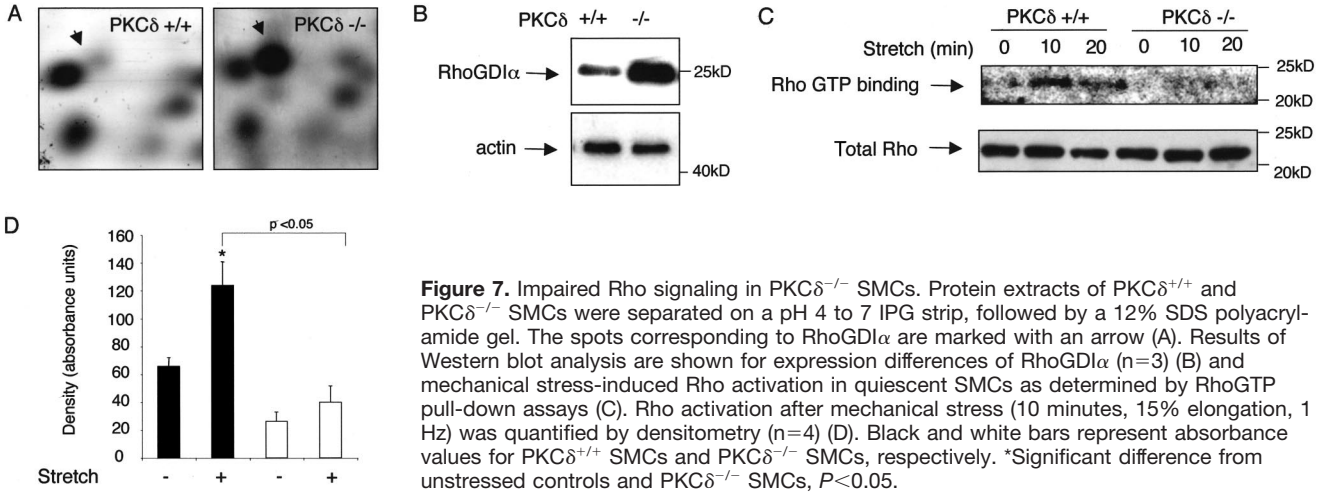

Figure 7. Impaired Rho signaling in PKC$\delta^{-/-}$ SMCs. Protein extracts of PKC$\delta^{+/+}$ and PKC$\delta^{-/-}$ SMCs were separated on a pH 4 to 7 IPG strip, followed by a 12% SDS polyacrylamide gel. The spots corresponding to RhoGDIα are marked with an arrow (A). Results of Western blot analysis are shown for expression differences of RhoGDIα (n=3) (B) and mechanical stress-induced Rho activation in quiescent SMCs as determined by RhoGTP pull-down assays (C). Rho activation after mechanical stress (10 minutes, 15% elongation, 1 Hz) was quantified by densitometry (n=4) (D). Black and white bars represent absorbance values for PKC$\delta^{+/+}$ SMCs and PKC$\delta^{-/-}$ SMCs, respectively. *Significant difference from unstressed controls and PKC$\delta^{-/-}$ SMCs, $P<0.05$.

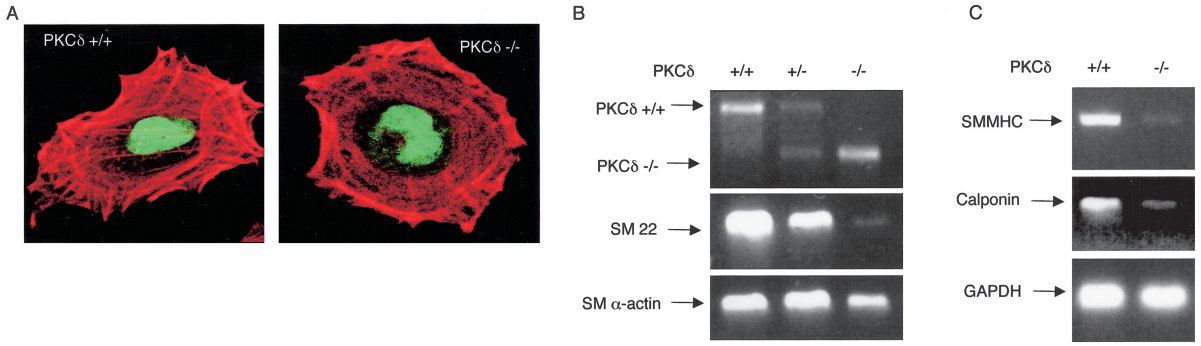

Figure 8. Loss of PKCδ results in SMC dedifferentiation. Actin fiber formation during cell spreading as visualized by rhodamine phalloidin staining (A). Absence of PKCδ in cultivated SMCs as confirmed by PCR (B, upper panel). RT-PCR data showing decreased expression of SMC differentiation markers in PKCδ$^{-/-}$ SMCs (n=5 for PKCδ$^{+/+}$ and PKCδ$^{-/-}$ SMCs, n=2 for PKCδ$^{+/-}$ SMCs) (B, C).

preferentially converted to phospholipids if they escape mitochondrial oxidation. Aldehyde dehydrogenases catalyze the oxidation of medium and long-chain fatty aldehydes to their corresponding carboxylic acids. Acyl-CoA dehydrogenases are responsible for β-oxidation of short chain fatty acids. Second, the pentose phosphate pathway can account for complete oxidation of glucose, the main products being NADPH and CO_2. All tissues in which this pathway is active use NADPH in reductive synthesis including synthesis of GSH.[37] Glucose 6-phosphate dehydrogenase is the first and rate-limiting enzyme in the pentose phosphate pathway. Two other $NADP^+$-linked dehydrogenases contribute to the generation of cytosolic NADPH, malic enzyme, and cytoplasmic isocitrate dehydrogenase.[17,38] Both glucose 6-phosphate dehydrogenase and cytoplasmic isocitrate dehydrogenase were altered in our proteomic analysis of PKCδ$^{-/-}$ SMCs. Thus, PKCδ-associated changes in glucose metabolism appear to contribute to an increase in GSH, which plays an essential role in maintaining cellular redox balance.

Another important observation of this study is the upregulation of RhoGDIα, an endogenous inhibitor of Rho signaling pathways, which was associated with cytoskeletal abnormalities and a phenotypic modulation in PKCδ$^{-/-}$ SMCs. Rho signaling is a key regulator of SMC differentiation.[30] SMC-specific markers are regulated at a transcriptional level. Except for α-SM actin, transcription of these genes is downregulated in dedifferentiated SMCs. Loss of PKCδ coincided with decreased expression of SMC differentiation markers, including SM22, SMMHC, and calponin, suggesting that PKCδ is required for maintaining SMC differentiation.

Hemodynamic forces are known to be instrumental in the pathogenesis of vein graft stenosis.[39] We have demonstrated previously that mechanical stress can induce SMC apoptosis in vivo and in vitro.[26,27,40,41] Two signaling pathways appear to be involved in initiating SMC apoptosis after mechanical stress: Rac/p38 MAPK activation and oxidative DNA damage.[26,27] These findings were subsequently confirmed by others.[42–44] Importantly, enhanced apoptosis after mechanical injury is associated with a decrease in GSH levels,[45] and the response of SMCs to mechanical strain is modulated by glucose 6-phosphate dehydrogenase activity.[23] Therefore, our mechanistic data provide a better explanation of why PKCδ$^{-/-}$ SMCs are resistant to apoptosis and contribute to accelerated neointima formation in PKCδ$^{-/-}$ vein grafts.

In summary, the present study provides new insights into PKCδ isoform specific effects, which could not have been obtained by studying individual signaling pathways. Our integrated approach highlights the intimate connections between glucose metabolism and susceptibility to cell death, and identifies PKCδ as one of the key kinases in vascular SMCs, ideally positioned to serve as a "sentinel" responding to abnormalities in glucose metabolism, oxidative stress, and cytoskeleton rearrangement. Our findings highlight potential targets for gene or drug therapy, because enhanced PKCδ induction in the vessel wall could reduce neointima formation by promoting SMC apoptosis and maintaining SMC differentiation after mechanical injury.

Acknowledgments

This work was supported by grants from British Heart Foundation (PG/02/234/13592) and the Oak Foundation. The use of the facilities of the Medical Biomics Centre at St George's Hospital Medical School and the help of Dr Robin Wait (Imperial College, London, UK) are gratefully acknowledged.

References

1. McGregor E, Dunn MJ. Proteomics of heart disease. *Hum Mol Genet*. 2003;12:R135–R144.
2. Loscalzo J. Proteomics in cardiovascular biology and medicine. *Circulation*. 2003;108:380–383.
3. Lopez MF, Melov S. Applied proteomics: mitochondrial proteins and effect on function. *Circ Res*. 2002;90:380–389.
4. Huber LA, Pfaller K, Vietor I. Organelle proteomics: implications for subcellular fractionation in proteomics. *Circ Res*. 2003;92:962–968.
5. Fan TW, Higashi RM, Lane AN, Jardetzky O. Combined use of 1H-NMR and GC-MS for metabolite monitoring and in vivo 1H-NMR assignments. *Biochim Biophys Acta*. 1986;882:154–167.
6. Arrell DK, Neverova I, Van Eyk JE. Cardiovascular proteomics: evolution and potential. *Circ Res*. 2001;88:763–773.
7. Bonow R, Clark EB, Curfman GD, Guttmacher A, Hill MN, Miller DC, Morrison AR, Myerburg RJ, Schneider MD, Weisfeldt ML, Willerson JT, Young JB. Task Force on Strategic Research Direction: Clinical Science Subgroup key science topics report. *Circulation*. 2002;106:e162–e166.
8. Patton WF, Erdjument-Bromage H, Marks AR, Tempst P, Taubman MB. Components of the protein synthesis and folding machinery are induced in vascular smooth muscle cells by hypertrophic and hyperplastic agents. Identification by comparative protein phenotyping and microsequencing. *J Biol Chem*. 1995;270:21404–21410.
9. Kikkawa U, Matsuzaki H, Yamamoto T. Protein Kinase Cdelta (PKC-delta): Activation Mechanisms and Functions. *J Biochem (Tokyo)*. 2002; 132:831–839.

10. Ron D, Kazanietz MG. New insights into the regulation of protein kinase C and novel phorbol ester receptors. *FASEB J*. 1999;13:1658–1676.
11. Leitges M, Mayr M, Braun U, Mayr U, Li C, Pfister G, Ghaffari-Tabrizi N, Baier G, Hu Y, Xu Q. Exacerbated vein graft arteriosclerosis in protein kinase Cdelta-null mice. *J Clin Invest*. 2001;108:1505–1512.
12. Mayr U, Mayr M, Li C, Wernig F, Dietrich H, Hu Y, Xu Q. Loss of p53 accelerates neointimal lesions of vein bypass grafts in mice. *Circ Res*. 2002;90:197–204.
13. Li C, Wernig F, Leitges M, Hu Y, Xu Q. Mechanical stress-activated PKCdelta regulates smooth muscle cell migration. *FASEB J*. 2003;17: 2106–2108.
14. Hu Y, Zou Y, Dietrich H, Wick G, Xu Q. Inhibition of neointima hyperplasia of mouse vein grafts by locally applied suramin. *Circulation*. 1999;100:861–868.
15. McGregor E, Kempster L, Wait R, Welson SY, Gosling M, Dunn MJ, Powel JT. Identification and mapping of human saphenous vein medial smooth muscle proteins by two-dimensional polyacrylamide gel electrophoresis. *Proteomics*. 2001;1:1405–1414.
16. Bergmeyer H. *Methods of enzymatic analysis.* Weinheim, Germany: Verlag Chemie; 1974.
17. Lee SM, Koh HJ, Park DC, Song BJ, Huh TL, Park JW. Cytosolic NADP(+)-dependent isocitrate dehydrogenase status modulates oxidative damage to cells. *Free Radic Biol Med*. 2002;32:1185–1196.
18. Roobol A, Sahyoun ZP, Carden MJ. Selected subunits of the cytosolic chaperonin associate with microtubules assembled in vitro. *J Biol Chem*. 1999;274:2408–2415.
19. Lundstrom J, Holmgren A. Determination of the reduction-oxidation potential of the thioredoxin-like domains of protein disulfide-isomerase from the equilibrium with glutathione and thioredoxin. *Biochemistry*. 1993;32:6649–6655.
20. Lumb RA, Bulleid NJ. Is protein disulfide isomerase a redox-dependent molecular chaperone? *EMBO J*. 2002;21:6763–6770.
21. Powell LA, Nally SM, McMaster D, Catherwood MA, Trimble ER. Restoration of glutathione levels in vascular smooth muscle cells exposed to high glucose conditions. *Free Radic Biol Med*. 2001;31:1149–1155.
22. Tachi Y, Okuda Y, Bannai C, Okamura N, Bannai S, Yamashita K. High concentration of glucose causes impairment of the function of the glutathione redox cycle in human vascular smooth muscle cells. *FEBS Lett*. 1998;421:19–22.
23. Leopold JA, Loscalzo J. Cyclic strain modulates resistance to oxidant stress by increasing G6PDH expression in smooth muscle cells. *Am J Physiol Heart Circ Physiol*. 2000;279:H2477–H2485.
24. Hancock JF, Hall A. A novel role for RhoGDI as an inhibitor of GAP proteins. *EMBO J*. 1993;12:1915–1921.
25. Ridley A. Rac and Rho. *Curr Biol*. 1999;9:R156.
26. Mayr M, Li C, Zou Y, Huemer U, Hu Y, Xu Q. Biomechanical stress-induced apoptosis in vein grafts involves p38 mitogen-activated protein kinases. *FASEB J*. 2000;14:261–270.
27. Mayr M, Hu Y, Hainaut H, Xu Q. Mechanical stress-induced DNA damage and rac-p38MAPK signal pathways mediate p53-dependent apoptosis in vascular smooth muscle cells. *FASEB J*. 2002;16:1423–1425.
28. Li C, Hu Y, Sturm G, Wick G, Xu Q. Ras/Rac-Dependent activation of p38 mitogen-activated protein kinases in smooth muscle cells stimulated by cyclic strain stress. *Arterioscler Thromb Vasc Biol*. 2000;20:E1–E9.
29. Worth NF, Rolfe BE, Song J, Campbell GR. Vascular smooth muscle cell phenotypic modulation in culture is associated with reorganisation of contractile and cytoskeletal proteins. *Cell Motil Cytoskeleton*. 2001;49: 130–145.
30. Mack CP, Somlyo AV, Hautmann M, Somlyo AP, Owens GK. Smooth muscle differentiation marker gene expression is regulated by RhoA-mediated actin polymerization. *J Biol Chem*. 2001;276:341–347.
31. Zeidan A, Nordstrom I, Albinsson S, Malmqvist U, Sward K, Hellstrand P. Stretch-induced contractile differentiation of vascular smooth muscle: sensitivity to actin polymerization inhibitors. *Am J Physiol Cell Physiol*. 2003;284:C1387–C1396.
32. Frasch SC, Henson PM, Kailey JM, Richter DA, Janes MS, Fadok VA, Bratton DL. Regulation of phospholipid scramblase activity during apoptosis and cell activation by protein kinase Cdelta. *J Biol Chem*. 2000; 275:23065–23073.
33. Caruso M, Maitan MA, Bifulco G, Miele C, Vigliotta G, Oriente F, Formisano P, Beguinot F. Activation and mitochondrial translocation of protein kinase Cdelta are necessary for insulin stimulation of pyruvate dehydrogenase complex activity in muscle and liver cells. *J Biol Chem*. 2001;276:45088–45097.
34. Soltoff SP. Rottlerin is a mitochondrial uncoupler that decreases cellular ATP levels and indirectly blocks protein kinase Cdelta tyrosine phosphorylation. *J Biol Chem*. 2001;276:37986–37992.
35. Paul RJ, Krisanda JM, Lynch RM. Vascular smooth muscle energetics. *J Cardiovasc Pharmacol*. 1984;6:S320–S327.
36. Lynch RM, Paul RJ. Compartmentation of glycolytic and glycogenolytic metabolism in vascular smooth muscle. *Science*. 1983;222:1344–1346.
37. Jain M, Brenner DA, Cui L, Lim CC, Wang B, Pimentel DR, Koh S, Sawyer DB, Leopold JA, Handy DE, Loscalzo J, Apstein CS, Liao R. Glucose-6-phosphate dehydrogenase modulates cytosolic redox status and contractile phenotype in adult cardiomyocytes. *Circ Res*. 2003;93: e9–16.
38. Jo SH, Son MK, Koh HJ, Lee SM, Song IH, Kim YO, Lee YS, Jeong KS, Kim WB, Park JW, Song BJ, Huh TL, Huhe TL. Control of mitochondrial redox balance and cellular defense against oxidative damage by mitochondrial NADP+-dependent isocitrate dehydrogenase. *J Biol Chem*. 2001;276:16168–16176.
39. Xu Q. Biomechanical-stress-induced signaling and gene expression in the development of arteriosclerosis. *Trends Cardiovasc Med*. 2000;10: 35–41.
40. Mayr M, Xu Q. Smooth muscle cell apoptosis in arteriosclerosis. *Exp Gerontol*. 2001;36:969–987.
41. Wernig F, Xu Q. Mechanical stress-induced apoptosis in cardiovascular system. *Progress Biophys Mol Biol*. 2002;78:105–137.
42. Sotoudeh M, Li YS, Yajima N, Chang CC, Tsou TC, Wang Y, Usami S, Ratcliffe A, Chien S, Shyy JY. Induction of apoptosis in vascular smooth muscle cells by mechanical stretch. *Am J Physiol Heart Circ Physiol*. 2002;282:H1709–H1716.
43. Cornelissen J, Armstrong J, Holt CM. Mechanical stretch induces phosphorylation of p38-MAPK and apoptosis in human saphenous vein. *Arterioscler Thromb Vasc Biol*. 2004;24:451–456.
44. Goldman J, Zhong L, Liu SQ. Degradation of alpha-actin filaments in venous smooth muscle cells in response to mechanical stretch. *Am J Physiol Heart Circ Physiol*. 2003;284:H1839–H1847.
45. Pollman MJ, Hall JL, Gibbons GH. Determinants of vascular smooth muscle cell apoptosis after balloon angioplasty injury. Influence of redox state and cell phenotype. *Circ Res*. 1999;84:113–121.

Material. Antibodies to RhoGDIα were purchased from Zymogen (50-100, dilution 1:500). All other antibodies were products from Santa Cruz: HO-1 (H-105, dilution 1:200), actin (I-19, 1:200). Anti-Rho antibodies were supplied with the Rho activation kits and used at the recommended concentrations (Upstate, Pierce).

Smooth muscle cell culture SMCs were cultured in DMEM (25 mM glucose, Gibco) supplemented with 15% fetal calf serum, penicillin (100 U/ml), and streptomycin (100 μg/ml). Cells were incubated at 37°C in a humidified atmosphere of 5% CO_2 and passaged by treatment with 0.05% trypsin / 0.02% EDTA solution. For cell signalling, SMCs were made quiescent by serum starvation for 3 days. For ATP and GSH measurements as well as experiments related to oxidative stress, SMCs were also cultivated in normoglucose medium (5mM, Sigma). The purity of SMCs was routinely confirmed by immunostaining with antibodies against α-actin. Experiments were conducted on SMCs achieving subconfluence at passages 15 to 35.

Two-dimensional gel electrophoresis (2-DE). SMCs were homogenised in lysis buffer (9.5 M urea, 2% w/v CHAPS. 0.8% w/v Pharmalyte, pH 3-10 and 1% w/v DTT) containing a cocktail of protease inhibitors (Complete Mini, Roche) and centrifuged at 13,000 g at 20°C for 10 min. A minor pellet containing insoluble proteins remained after lysis in urea buffer and subsequent centrifugation. The supernatant containing soluble proteins was harvested and protein concentration was determined [1] using a modification of the method described by Bradford [2]. Solubilised samples were divided into aliquots and stored at –80°C. For two-dimensional gel electrophoresis (2-DE), extracts were loaded on nonlinear immobilized pH gradient 18-cm strips, 3-10 (Amersham Pharmacia Biotech.). For analytical and preparative gels, respectively, a protein load of 100 μg and 400 μg was applied to each IPG strip using an in-gel rehydration method. Samples were diluted in rehydration solution (8

M urea, 0.5% w/v CHAPS, 0.2% w/v DTT, and 0.2 % w/v Pharmalyte pH 3-10) and rehydrated overnight in a reswelling tray. Strips were focussed at 0.05 mA/IPG strip for 60 kVh at 20°C. Once IEF was completed the strips were equilibrated in 6M urea containing 30% v/v glycerol, 2% w/v SDS and 0.01% w/v Bromphenol blue, with addition of 1% w/v DTT for 15 min, followed by the same buffer without DTT, but with the addition of 4.8% w/v iodoacetamide for 15 min. SDS-PAGE was performed using 12% T, 2.6% C separating polyacrylamide gels without a stacking gel, using the Ettan DALT system (Amersham). The second dimension was terminated when the Bromphenol dye front had migrated off the lower end to the gels. After electrophoresis, gels were fixed overnight in methanol: acetic acid: water solution (4:1:5 v/v/v). 2-DE protein profiles were visualised by silver staining using the Plus one silver staining kit (Amersham Pharmacia Biotech.) with slight modifications to ensure compatibility with subsequent mass spectrometry analysis. For image analysis, silver-stained gels were scanned in transmission scan mode using a calibrated scanner (GS-800, Biorad). Raw 2-DE gels were analysed using the PDQuest Software (Biorad). Normalization was performed for total spot number/volume. Differences were confirmed by an automated analysis software (Proteomeweaver, Definiens). For the present study, 8 gels were processed in parallel to guarantee a maximum of comparability. Each 2-DE run was at least repeated once. All 2-DE gels were of high quality in terms of resolution as well as consistency in spot patterns. A molecular weight and pI grid was computed based on the identification of 200 spots (Mayr et al, unpublished data) using the PDQuest Software.

Mass spectrometry. Gel pieces containing selected protein spots were treated overnight with modified trypsin (Promega) according to a published protocol [3].

Peptide fragments were recovered by sequential extractions with 50mM ammonium hydrogen carbonate, 5% v/v formic acid, and acetonitrile. Extracts were lyophilized, resuspended in 20 μl of 0.1% v/v TFA/ 10% v/v acetonitrile, and desalted on Zip tips (Millipore) according to the manufacturer's instruction. MALDI-MS was performed using an Axima CFR spectrometer (Kratos, Manchester, UK). The instrument was operated in the positive ion reflectron mode. □-cyano-4-hydroxy-cinnaminic acid was applied as matrix. Spectra were internally calibrated using trypsin autolysis products. The resulting peptide masses were searched against databases using the MASCOT program [4]. One missed cleavage per peptide was allowed and carbamidomethylation of cysteine as well as partial oxidation of methionine were assumed. In addition to MALDI-MS, tandem mass spectrometry was performed for sequencing of tryptic digest peptides. Following enzymatic degradation, peptides were separated by capillary liquid chromatography on a reverse-phase column (BioBasic-18, 100 x 0.18 mm, particle size 5 μm, Thermo Electron Corporation) and applied to a LCQ ion-trap mass spectrometer (LCQ Deca XP Plus, Thermo Finnigan). Spectra were collected from the ion-trap mass analyzer using full ion scan mode over the mass-to-charge (m/z) range 300-2000. MS-MS scans were performed on each ion using dynamic exclusion. Database search was performed using the TurboSEQUEST software (Thermo Finnigan).

ATP and GSH measurements. Intracellular ATP and total glutathione levels were determined by spectroscopy as described previously[5,6].

Cell viability assay. For cell viability assays, SMCs (2 x 10^3) were cultured in 96-well plates. After 24 h, cells were incubated with diethylmaleate (DEM). A solution (Aqueous One Solution Cell Proliferation Assay, Promega) was added 2 h

before the end of the incubation period and the optical density at 490 nm was recorded by photometry[7].

Western Blotting and kinase assays. Cellular protein extracts were harvested according to an established protocol[8,9]. Western blotting was performed as described previously[8,9].

Rho activation assay. SMCs were seeded on silicone elastomer-bottomed culture plates (Flexcell, McKeesport, PA) at $1.5x10^5$ cells per well, grown for 48 h, and subjected to cyclic strain. The Cyclic Stress Unit, a modification of the unit initially described by Banes et al[10], consisted of a computer-controlled vacuum unit and a base plate to hold the culture plates (FX3000 AFC-CTL, Flexcell). A vacuum (15 to 20kPa) was repetitively applied to the elastomer-bottomed plates via the base plate. Cyclic deformation (60 cycles/min) with 15% elongation was applied for up to 20 min in a humidified incubator with 5% CO_2 at 37°C. Rho activation was measured by RhoGTP pull-down assays using two commercial kits (Pierce and Upstate).

Cell spreading assay. SMC were plated on a slide bottle and cultured in DMEM supplemented with 20% FCS at 37°C in a humidified atmosphere with 5% CO_2. After 6h, cells were washed with cold phosphate buffered saline (PBS), fixed for 15 min at room temperature (2% formaldehyde, 0.2% glutaraldehyde in PBS, pH 7.2), treated with 0.02% Triton X-100 in PBS for 2 min, washed with PBS and then blocked with 1% bovine serum albumin (BSA) in PBS. For actin staining, cells were incubated with rhodamine phalloidin (Sigma) for 30 min[11]. Counterstaining of cell nuclei was performed with Sytox-Green (5 μM, Molecular Probes) for 20 min.

RT-PCR. Total RNA was extracted using the Fast RNA kit according to the protocol provided by the manufacturer (Qiagen). 2 μg of total RNA was reverse transcribed into complementary DNA (cDNA) using the Promega reverse

transcription system. The RT products were examined by PCR with primers for SMC differentiation markers as described previously[12].

References:

1. Weekes J, Wheeler CH, Yan JX, Weil J, Eschenhagen T, Scholtysik G, Dunn MJ. Bovine dilated cardiomyopathy: proteomic analysis of an animal model of human dilated cardiomyopathy. *Electrophoresis*. 1999;20:898-906.
2. Bradford MM. A rapid and sensitive method for the quantitation of microgram quantities of protein utilizing the principle of protein-dye binding. *Anal Biochem*. 1976;72:248-54.
3. Shevchenko A, Wilm M, Vorm O, Mann M. Mass spectrometric sequencing of proteins silver-stained polyacrylamide gels. *Anal Chem*. 1996;68:850-8.
4. Perkins DN, Pappin DJ, Creasy DM, Cottrell JS. Probability-based protein identification by searching sequence databases using mass spectrometry data. *Electrophoresis*. 1999;20:3551-67.
5. Jenner AM, Ruiz JE, Dunster C, Halliwell B, Mann GE, Siow RC. Vitamin C protects against hypochlorous Acid-induced glutathione depletion and DNA base and protein damage in human vascular smooth muscle cells. *Arterioscler Thromb Vasc Biol*. 2002;22:574-80.
6. Ruiz E, Siow RC, Bartlett SR, Jenner AM, Sato H, Bannai S, Mann GE. Vitamin C inhibits diethylmaleate-induced L-cystine transport in human vascular smooth muscle cells. *Free Radic Biol Med*. 2003;34:103-10.
7. Mayr U, Mayr M, Li C, Wernig F, Dietrich H, Hu Y, Xu Q. Loss of p53 accelerates neointimal lesions of vein bypass grafts in mice. *Circ Res*. 2002;90:197-204.
8. Li C, Hu Y, Mayr M, Xu Q. Cyclic strain stress-induced mitogen-activated protein kinase (MAPK) phosphatase 1 expression in vascular smooth muscle cells is regulated by Ras/Rac-MAPK pathways. *J Biol Chem*. 1999;274:25273-80.
9. Li C, Hu Y, Sturm G, Wick G, Xu Q. Ras/Rac-Dependent activation of p38 mitogen-activated protein kinases in smooth muscle cells stimulated by cyclic strain stress. *Arterioscler Thromb Vasc Biol*. 2000;20:E1-9.
10. Banes AJ, Gilbert J, Taylor D, Monbureau O. A new vacuum-operated stress-providing instrument that applies static or variable duration cyclic tension or compression to cells in vitro. *J Cell Sci*. 1985;75:35-42.
11. Li C, Wernig F, Leitges M, Hu Y, Xu Q. Mechanical stress-activated PKCdelta regulates smooth muscle cell migration. *Faseb J*. 2003.
12. Hu Y, Davison F, Ludewig B, Erdel M, Mayr M, Url M, Dietrich H, Xu Q. Smooth muscle cells in transplant atherosclerotic lesions are originated from recipients, but not bone marrow progenitor cells. *Circulation*. 2002;106:1834-9.